Proc. NIPR Symp. Antarct. Meteorites, 7, 9–29, 1994

PETROGRAPHY AND PETROLOGY OF THE ALH-77005 SHERGOTTITE

Yukio IKEDA

Department of Earth Sciences, Faculty of Science, Ibaraki University, 1–1, Bunkyo 2-chome, Mito 310

Abstract: The ALH-77005 shergottite is a cumulate gabbroic rock consisting of brown olivine, low- and high-Ca pyroxene, plagioclase glass, Ti-poor and -rich chromite, ilmenite, whitlockite, and sulfides. Chromites in ALH-77005 show four types of chemical zoning, and these types suggest multiple magma mixing. Some plagioclase glass has plagioclase rims, and the rims were produced from plagioclase melts by rapid crystallization. Ubiquitous occurrences of plagioclase glass and shock-melt pockets that were produced by *in-situ* melting indicate that ALH-77005 has experienced shock pressures ranging from 50 to 80 GPa.

1. Introduction

The ALH-77005 meteorite (this name is used in Catalog of Japanese Collection of the Antarctic Meteorites, whereas ALHA77005 is used in Antarctic Meteorite Newsletter) is a unique shergottite, showing a cumulative gabbroic texture, which differs in texture and mineral composition from other basaltic and doleritic shergottites (MCSWEEN *et al.*, 1979a). It shows the most intense shock effects among all of the SNC meteorites, which are considered to have experienced varying degrees of shock impact when they were ejected from Mars (BOGARD *et al.*, 1984; MCSWEEN, 1984, 1985).

The petrology and shock features of ALH-77005 have already been studied by some authors (MCSWEEN *et al.*, 1979a, b; MCSWEEN and STOFFLER, 1980; SHIH *et al.*, 1982; SMITH and STEELE, 1984; OSTERTAG *et al.*, 1984; STOFFLER *et al.*, 1986; JAGOUTZ, 1989; LONGHI and PAN, 1989; LUNDBERG *et al.*, 1990; BISCHOFF and STOFFLER, 1992). MCSWEEN *et al.* (1979a, b) showed that ALH-77005 has unique cumulate textures and mineral compositions different from other shergottites, but has a close genetic relationship with them. He suggested that ALH-77005 might be a cumulate that crystallized from a liquid parental to those from which the shergottites crystallized, or it might be a sample of the type of peridotite from which shergottite parent magmas were derived by partial melting. Their REE study also supported a genetic relationship between ALH-77005 and Shergotty (MA *et al.*, 1981). LUNDBERG *et al.* (1990) showed that ALH-77005 includes about 50% cumulus material (olivine and chromite) and the intercumulus liquid crystallized as a closed system to form successively poikilitic low-Ca and high-Ca pyroxene,

followed by interstitial pyroxene, plagioclase, and whitlockite. Shock features in ALH-77005 were first studied by MCSWEEN and STOFFLER (1980); irregular shock-melt pockets and pseudotachylite veins comprise up to 20% by volume of the meteorite. The maskelynite has the lowest refractive index (1.530 ± 0.002) among the shergottites, some maskelynite has been converted to single-crystal plagioclase with undulatory extinction, and the pyroxene and olivine exhibit strong mosaicism and a variety of planar deformation structures. These shock features in ALH-77005 indicate that the degree of shock metamorphism requires shock pressures in the range of 35 to 50 GPa, with a probable equilibrium peak pressure of 45 GPa (MCSWEEN and STOFFLER, 1980). STOFFLER *et al.* (1986) concluded that the equilibrium shock pressure and post-shock temperature for ALH-77005 are 43 ± 2 GPa and 400–800°C, respectively. Brown colored olivine is characteristic of ALH-77005 (MCSWEEN and STOFFLER, 1980), and approximately 4.5 wt% of the total iron of the olivine is trivalent (OSTERTAG *et al.*, 1984). The color may be the result of shock-induced oxidation of the olivine crystals on the meteorite parent body (OSTERTAG *et al.*, 1984). Recently, LEW88516, which is very similar to ALH-77005, was found (HARVEY and MCSWEEN, 1992), although the former is more ferroan than the latter.

The purpose of this paper is to present more detailed petrography and mineralogy of the ALH-77005 shergottite, especially for chromite and "so called" maskelynite to discuss the formation of the meteorite.

2. Analytical Method

Chemical compositions of minerals were obtained with an electron-probe microanalyzer (EPMA, JEOL-Superprobe-733), and corrections were made by the Bence-Albee method for silicates, oxides, and phosphates, and the ZAF method for sulfides. The bulk compositions of shock-melt pockets and veins were obtained using a broad beam EPMA technique; the beam was about 40 microns across. Beam spot analyses were performed to cover an entire pocket for shock-melt pockets, and four or five beam spots were averaged for veins. The broad beam analysis correction technique of IKEDA (1980) was applied to shock-melt pockets and veins. Representative chemical compositions of minerals, shock-melt pockets, and veins are shown in Table 1, and those of sulfides in Table 2.

3. Petrography and Mineralogy

3.1. Overall petrographic features of ALH-77005

ALH-77005 is a gabbroic rock consisting of olivine, low-Ca pyroxene, high-Ca pyroxene, plagioclase glass with or without plagioclase rims, chromite, ilmenite, whitlockite, and pyrrhotite with pentlandite inclusions. The normative composition (MA *et al.*, 1981) is: 52% olivine, 26% low-Ca pyroxene, 11% high-Ca pyroxene, 10% plagioclase (or plagioclase glass), and 1% chromite. Two thin sections of ALH-77005 were used in this study, each being about 1 cm in diameter, and

Table 1. Representative chemical compositions of olivine, low-Ca pyroxene, augite, plagioclase (Pl) glass, plagioclase, chromite, ilmenite (Ilm), whitlockite (Whl), shock-melt pockets (P-1, P-2, P-3), shock-melt veins, quenched olivine (Q-Ol), quenched orthopyroxene (Q-Opx), and quenched augite (Q-Aug). The capital letters in the second line for pyroxene, plagioclase and glass, and chromite correspond to those in Figs. 3, 4, and 7. The chemical compositions of shock-melt pockets and veins were obtained by a broad beam of an EPMA.

	Olivine	low-Ca Pyroxene				Augite		Pl-glass		Plagioclase		Chromite			
		A	B	C	D	E	F	V	W	X	Y	A	B	C	D
SiO_2	37.51	55.20	54.29	53.11	53.65	52.87	50.70	53.40	53.75	54.05	54.23	0.03	0.00	0.01	0.00
TiO_2	0.00	0.05	0.23	0.54	0.80	0.30	1.50	0.05	0.00	0.04	0.03	0.80	1.18	0.86	1.33
Al_2O_3	0.02	0.42	0.72	1.02	1.01	1.46	2.28	27.60	27.49	28.06	28.30	7.37	9.11	5.68	8.03
Cr_2O_3	0.00	0.46	0.46	0.41	0.30	0.90	0.85	0.00	0.00	0.00	0.02	57.11	54.35	60.54	57.40
FeO	25.15	13.10	13.64	17.03	14.60	8.09	7.83	0.48	1.54	0.77	0.61	28.54	28.40	24.99	25.22
MnO	0.65	0.39	0.50	0.56	0.68	0.37	0.47	0.05	0.08	0.00	0.05	0.57	0.41	0.53	0.36
MgO	35.83	28.10	24.59	23.66	20.89	18.05	14.99	0.22	0.61	0.37	0.21	4.23	4.60	6.64	6.78
CaO	0.10	1.72	4.83	3.30	8.26	16.66	19.65	10.49	8.01	10.25	11.62	0.02	0.00	0.00	0.00
Na_2O	0.02	0.07	0.04	0.10	0.20	0.20	0.38	5.61	5.82	5.55	5.13	0.03	0.00	0.03	0.00
K_2O	0.00	0.00	0.00	0.00	0.00	0.00	0.00	0.31	0.72	0.08	0.07	0.00	0.00	0.00	0.00
P_2O_5															
Total	99.28	99.51	99.30	99.73	100.39	98.90	98.65	98.22	98.02	99.17	100.27	98.70	98.05	99.27	99.12

	Chromite			Ilm	Whl	Shock-melt pockets			Vein	Vein	Q-Ol	Q-Opx	Q-Aug
	E	F	G			P-1	P-2	P-3					
SiO_2	0.03	0.00	0.00	0.00	0.00	39.23	40.22	39.87	44.11	41.46	38.94	56.33	53.75
TiO_2	0.96	4.75	14.48	54.19	0.00	0.38	0.37	0.33	0.73	0.31	0.10	0.00	0.31
Al_2O_3	6.52	10.95	5.07	0.11	0.02	2.46	2.41	2.47	10.60	5.43	0.21	0.18	1.38
Cr_2O_3	57.84	45.04	30.93	0.59	0.15	1.14	0.78	0.82	0.60	0.57	0.68	0.56	0.86
FeO	28.72	31.06	42.92	37.99	0.84	23.60	21.61	22.88	15.04	20.54	15.18	9.53	8.26
MnO	0.45	0.50	0.46	0.67	0.00	0.43	0.40	0.44	0.23	0.32	0.24	0.39	0.32
MgO	4.62	5.72	4.36	5.48	3.09	30.19	30.52	29.40	14.81	26.99	44.22	32.33	19.97
CaO	0.01	0.10	0.00	0.00	47.13	2.13	2.94	3.02	8.15	3.15	0.22	0.56	14.85
Na_2O	0.03	0.00	0.02	0.00	1.03	0.43	0.39	0.40	1.54	1.01	0.08	0.08	0.09
K_2O	0.00	0.00	0.04	0.00	0.00	0.03	0.02	0.02	0.08	0.06	0.02	0.02	0.00
P_2O_5					46.66	0.25	0.36	0.34					
Total	99.18	98.13	98.24	99.03	98.92	100.27	100.02	99.99	98.52	100.03	99.89	99.98	99.80

The FeO is total Fe as FeO.

Table 2. Representative chemical compositions of pyrrhotite (Pyrr), and pyrrhotite including pentlandite grains (P + P).

	Pyrr	P+P
Fe	60.48	51.60
Ni	0.52	10.51
Co	0.18	0.58
Cu	0.06	0.00
Zn	0.04	0.00
S	37.85	37.76
Total	99.13	100.45

consisting of two portions bounded by a curvelinear or straight line: poikilitic and non-poikilitic portions. The poikilitic portion (Fig. 1a) comprises megacrystic low-Ca pyroxene grains, several mm in diameter, poikilitically including smaller corroded olivine grains, 0.1–1.0 mm across, with minor amounts of chromite, plagioclase glass, high-Ca pyroxene, and pyrrhotite. The non-poikilitic portion (Fig. 1c) consists of euhedral or subhedral olivine grains, 0.1–1.0 mm across, low- and high-Ca pyroxenes, and plagioclase glass, with minor amounts of chromite, ilmenite, whitlockite, and pyrrhotite.

All of the olivine and pyroxene had suffered intense shock, and their crystal structures had been modified in varying degrees, showing mosaic extinction under a microscope (Fig. 1b, d). Therefore, the constituent minerals are identified mainly by their chemical compositions.

3.2. *Olivine*

Olivine occurs as corroded grains in the poikilitic portion, and as euhedral or subhedral grains in the non-poikilitic portion. Quenched olivine in shock-melt pockets and veins (Fig. 1i, k, m, n, q, r) shows various shapes; rhombohedral, spinifex, lantern, or skeletal grains, of a few tens of microns in width and up to 100 microns in length. Olivine in the bulk of ALH-77005 has a brownish color, whereas the quenched olivine in shock-melt pockets and veins does not. The chemical composition of brown olivine is homogeneous within each grain, but changes from grain to grain, ranging from Fo_{70} to Fo_{75}. This homogeniety of olivine composition is considered to have been caused by re-equilibration with intercumulus liquid on cooling (LUNDBERG *et al.*, 1990). The MnO content of brown olivine is 0.4–0.7 wt% (Fig. 2). The quenched olivine in shock-melt pockets and veins shows remarkable chemical zoning from Fo_{86}–Fo_{58}.

3.3. *Pyroxene*

In the poikilitic portion of ALH-77005, low-Ca pyroxene occurs as large grains, about 5 mm across, including olivine grains (Fig. 1a). The large low-Ca pyroxenes show chemical zoning from CaO-poor magnesian cores (A in Fig. 3), via magnesian pigeonites (B in Fig. 3), to ferroan pigeonite rims (C in Fig. 3). There appears to be a compositional gap between pyroxenes A and B (Fig. 3). Low-Ca pyroxene in the

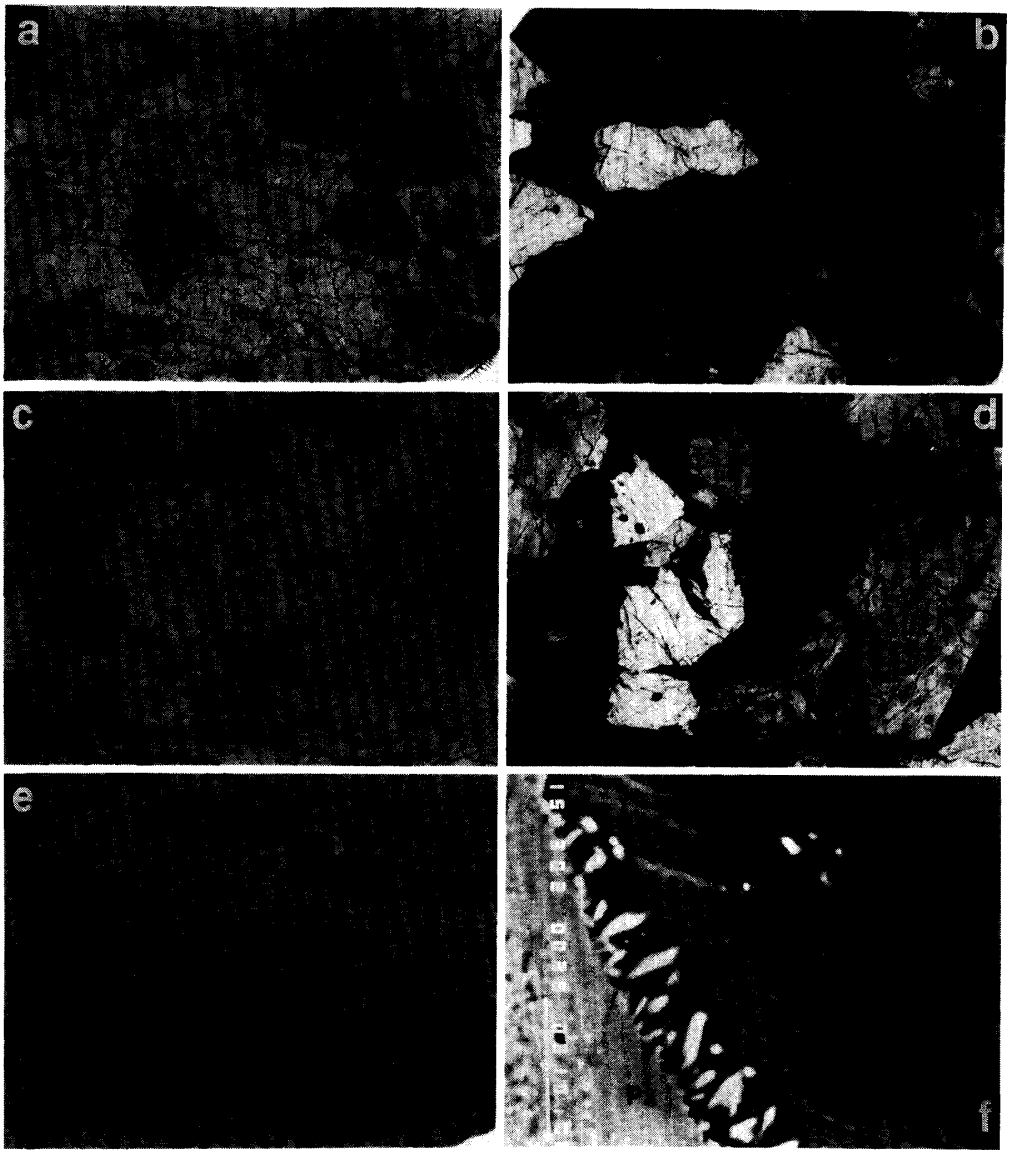

Fig. 1.

(a) Photomicrograph (transmitted light) of the poikilitic portion of ALH-77005. Note that brown olivine grains (Ol) with corroded outlines are included poikilitically in large low-Ca pyroxene grains (Px). Anhedral plagioclase glass (Pl, transparent) and euhedral chromite grains (black) occur in small amounts. Width is 2 mm.

(b) The same figure as (a) under crossed Nicols. Note that olivine and pyroxene show mosaic extinction.

(c) Photomicrograph (transmitted light) of the non-poikilitic portion of ALH-77005. Note that brown olivine occurs as subhedral grains sometimes just in contact with plagioclase glass, and is partly included in low-Ca pyroxene grains. Plagioclase glass, whitlockite (Wtl), ilmenite (Ilm), and chromite (Chm) occur as interstitial grains. Width is 2 mm.

(d) The same figure as (c) under crossed Nicols. Note that olivine and pyroxene show mosaic extinction although plagioclase and whitlockite have no birefringence.

(e) Photomicrograph (transmitted light) of plagioclase glass (Pl-gl) having plagioclase rims with compositional zoning (X, Y, and Z). Note that Becke's line between the plagioclase glass and the rims is clear, and that vesicles are found near the boundaries with the host olivine and pyroxene. Width is 150 microns.

(f) Back-scattered electron (BSE) image of the zoning of a plagioclase rim. Note that zone Z consists of cryptocrystalline intergrowth of pyroxene and plagioclase, and that euhedral pyroxene grains grow in zone Z from the host pyroxene wall. Width is 38 microns.

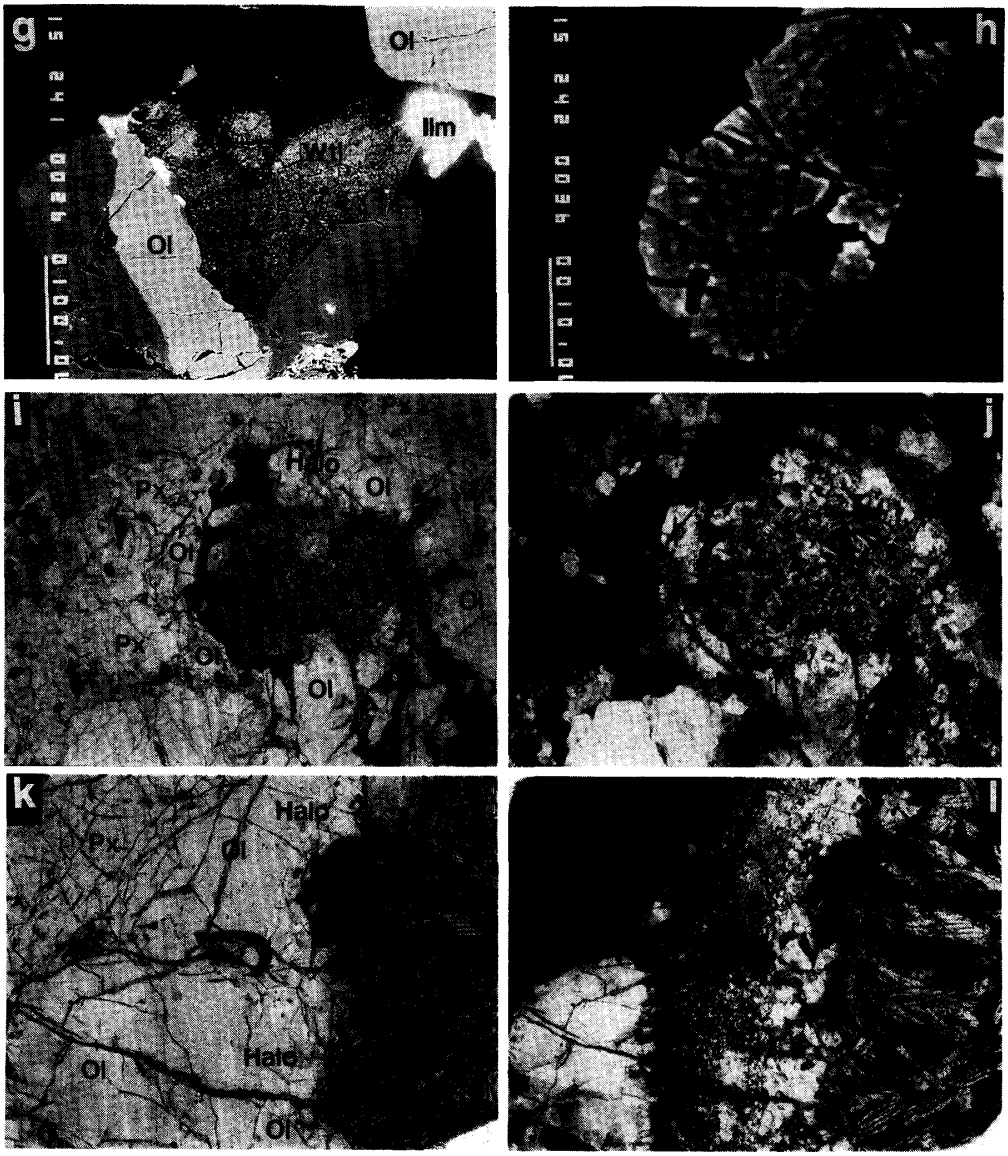

Fig. 1. (Continued)

(g) BSE image of whitlockite (Wtl) and ilmenite (Ilm) included in plagioclase glass (black), pyroxene (Px), and olivine (Ol). Note that the whitlockite grain has been broken, probably by a shock impact. Width is 450 microns.

(h) BSE image of pyrrhotite (gray) including small exsolved pentlandite grains (white). Width is 45 microns.

(i) Photomicrograph (transmitted light) of a shock-melt pocket. Note that the shock-melt pocket consists mainly of quenched olivine, which is coarser-grained in the center than in the periphery, and that olivine in the halo has lost the brownish color. Width is 3.7 mm.

(j) The same figure as (i) under crossed Nicols. Note that the halo shows a concentric extinction.

(k) Photomicrograph (transmitted light) of a halo surrounding a shock-melt pocket. Width is 1 mm.

(l) The same figure as (k) under crossed Nicols. Note that the inner portion of the halo is more severely broken, resulting in a concentric structure.

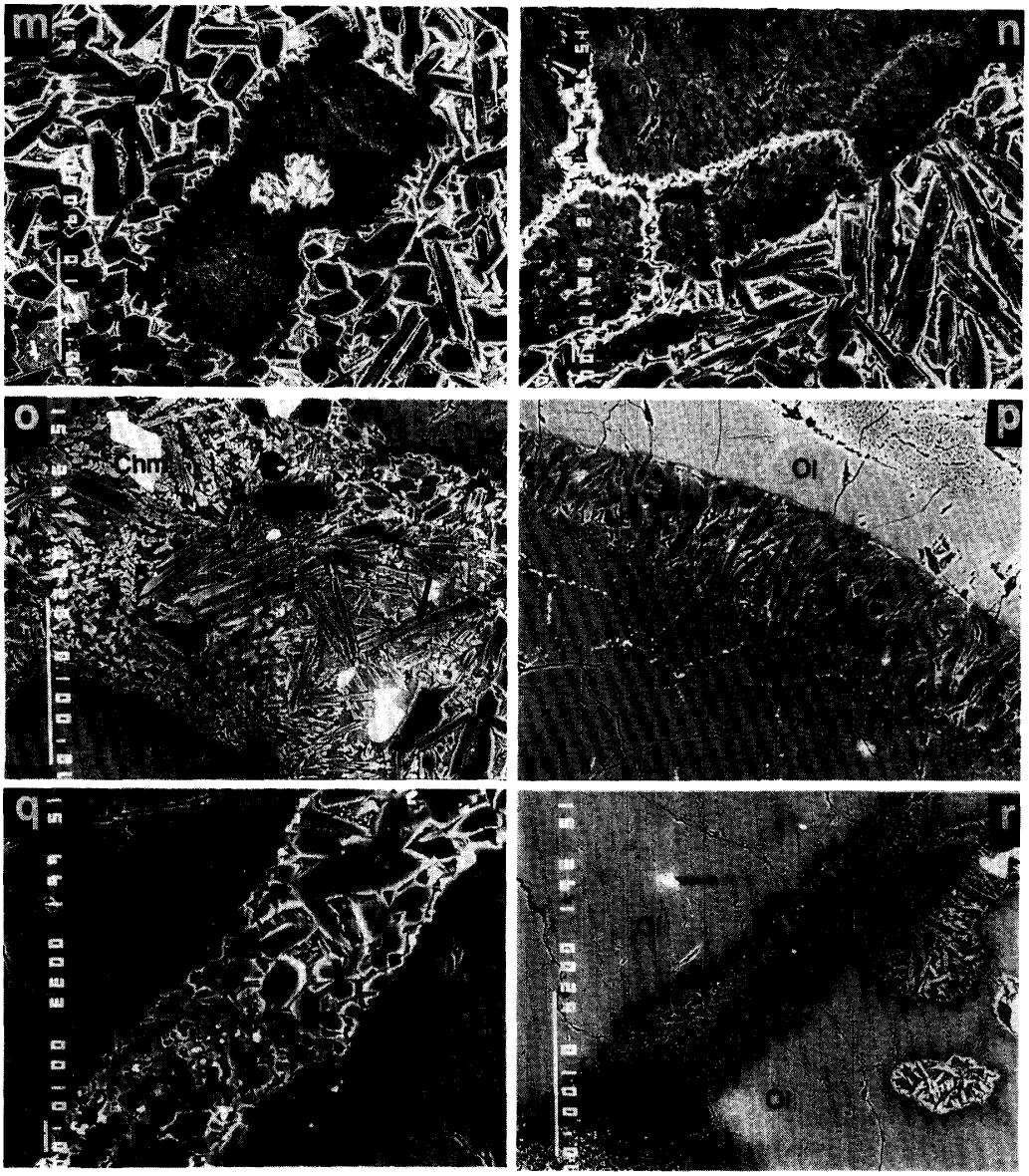

Fig. 1. (Continued)

(m) BSE image of a relic olivine grain in a shock-melt pocket. Note that the relic olivine grain consists of tiny ellipsoidal domains with chemical zoning from magnesian cores to ferroan rims, and that quenched euhedral olivine grains grow from the rim. Width is 450 microns.

(n) BSE image of a halo of a shock-melt pocket. Note that the inner portion of the halo shows a domain texture similar to that of relic olivine (m) in shock-melt pockets. Width is 210 microns.

(o) BSE image of a shock-melt vein. Note that quenched olivine grains, with spinifex, lantern, or skeletal shapes, and small pyroxene grains (gray) are set in the cryptocrystalline groundmass. A relic olivine grain (upper center) and chromite grains (white) occur in the vein. Width is 300 microns.

(p) BSE image of quenched augite grains (qAug) which grow directly from the host augite (Aug), suggesting that the quenched augite crystallized from an augite melt produced by "in situ" melting. Width is 170 microns.

(q) BSE image of a shock-melt vein consisting of euhedral olivine grains and interstitial cryptocrystalline groundmass. The host olivine in contact with the vein shows a domain texture. Width is 160 microns.

(r) BSE image of a shock-melt vein consisting of quenched olivine with lantern or spinefex shapes and interstitial cryptocrystalline groundmass. Width is 300 microns.

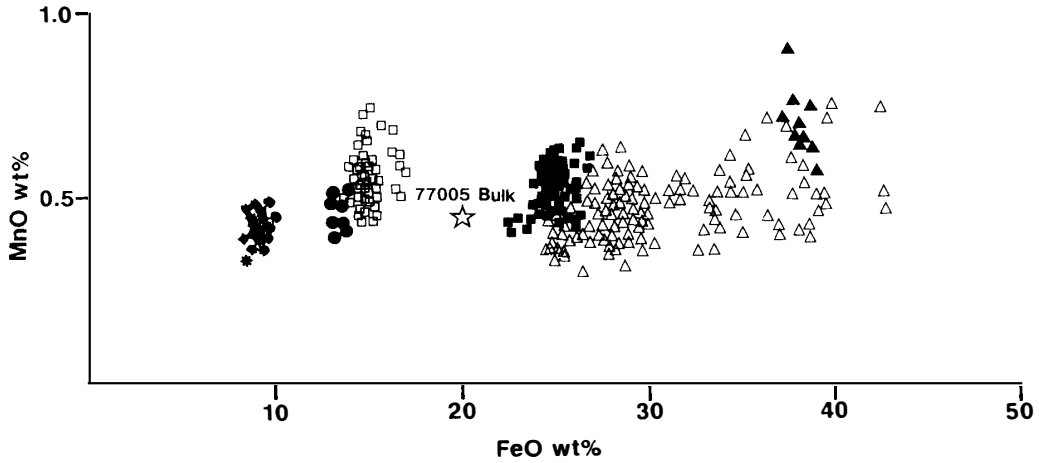

Fig. 2. The MnO contents of the minerals in ALH-77005 are plotted against the total FeO. Symbols are: brown olivine (solid square), orthopyroxene (closed circle), pigeonite (open square), augite (asterisk), chromite (open triangle), and ilmenite (closed triangle). The composition of the ALH-77005 whole rock (open star; SHIH et al., 1982) is shown for reference.

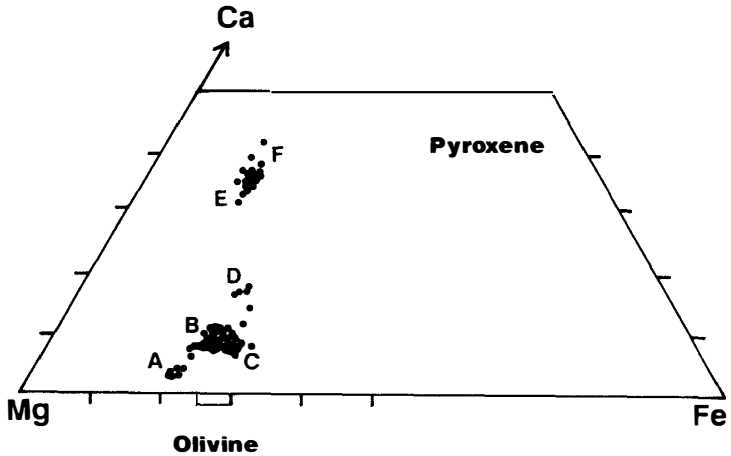

Fig. 3. The chemical compositions (in atomic %) of pyroxenes (closed circles; A, B, C, D, E, and F) and the compositional range of brown olivine (rectangular) in ALH-77005.

non-poikilitic portion is mainly magnesian pigeonite B, and ferroan pigeonite C occurs as rims on pigeonite B or as isolated euhedral crystals included in plagioclase glass. Low-Ca pigeonite with high Wo contents (D in Fig. 3) occurs in contact with whitlockite or ilmenite.

High-Ca pyroxene occurs in both the poikilitic and non-poikilitic portions and also shows chemical zoning from Ca-poor augite cores (E in Fig. 3) to Ca-rich augite rims (F in Fig. 3). Augite E often occurs in contact with pigeonite B, suggesting that they crystallized in close association with each other. There is no evidence for exsolution in pyroxenes.

The MnO contents of low-Ca pyroxene (Fig. 2) are 0.4–0.6 wt% for pyroxene

A and 0.4–0.8 wt% for B, C, and D. Those of high-Ca pyroxene are 0.3–0.5 wt% (Fig. 2).

3.4. Plagioclase glass (Pl-glass) and plagioclase

Pl-glass is present as pseudomorphs of the original plagioclase grains. It has been described as maskelynite in the literature, but has refractive indices lower than those of maskelynites in other shergottites (McSween and Stoffler, 1980; Stoffler *et al.*, 1986). As shown below, plagioclase rims crystallized after the formation of plagioclase melts by shock, and then the glass was quenched. Therefore, it is a glass rather than maskelynite (maskelynite is a diaplectic glassy material produced from plagioclase by shock without melting).

There are two types of Pl-glass, with and without plagioclase rims. Pl-glass without plagiolcase rims shows weak normal chemical zoning from anorthite (An)-rich cores (An_{50}–An_{55}) to An-poor rims (An_{45}–An_{50}), with an orthoclase (Or) content of about 1–2 mol%. Pl-glass with plagioclase rims tends to be located near shock-melt pockets, and one can easily recognize Becke lines between Pl-glass cores and plagioclase rims under a microscope (Fig. 1e). The crystalline plagioclase is not isotropic, when viewed with crossed Nicols. Pl-glass with plagioclase rims has remarkable and unusual chemical zoning. The core of Pl-glass is rich in An content (zone V in Figs. 4, 5; $An_{50-55}Or_{1-2}$), and the An content rapidly decreases toward the rims, which are enriched in albite (Ab) and Or components (zone W in Figs. 4, 5; $An_{40-45}Or_{2.5-5.0}$).

There is a compositional gap between Pl-glass cores and plagioclase rims. The

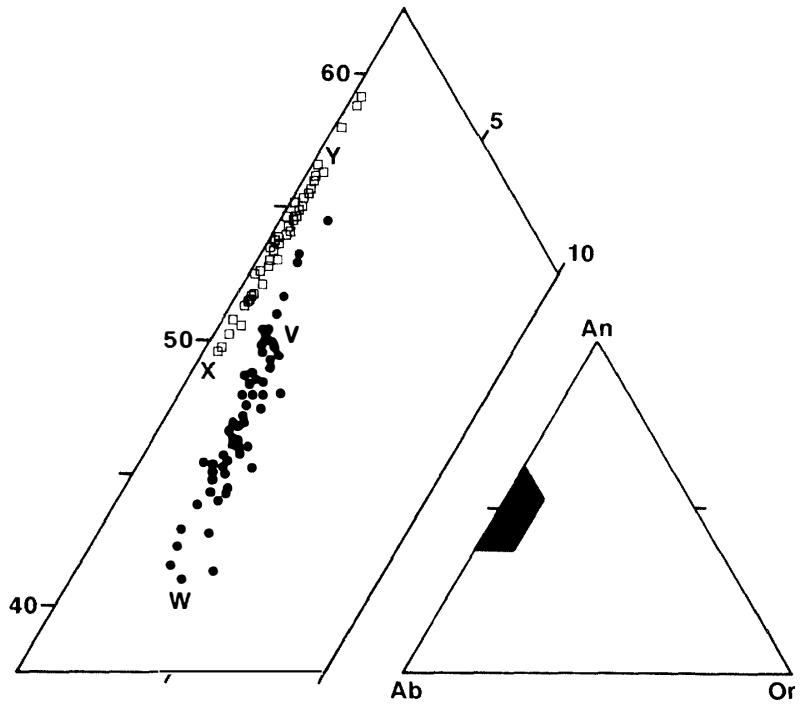

Fig. 4. Anorthite(An)-albite(Ab)-orthoclase(Or) mole ratios of plagioclase glass (closed circle) and plagioclase rims (open square) in ALH-77005. The capitals correspond to those in Fig. 5.

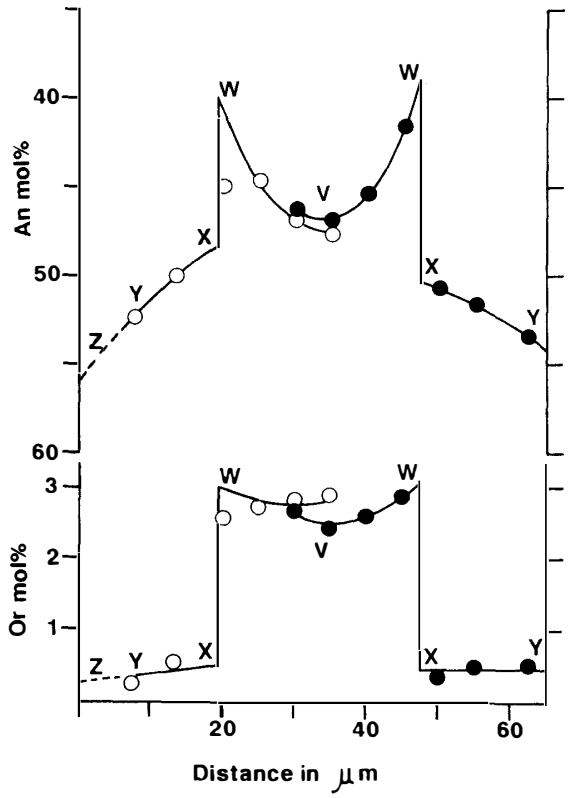

Fig. 5. Compositional zoning profiles of plagioclase glass with plagioclase rims in ALH-77005. The profile with open circles is a traverse from the host pyroxene, via a plagioclase rim (zones Z, Y, and X), to the plagioclase glass (zones W and V), the other profile with closed circles is a traverse from the host olivine, via a plagioclase rim (zones Y and X), to the plagioclase glass (zones W and V), and the two traverses are separated by distance of about a few tens of microns in the same plagioclase glass grain.

plagioclase rims change in composition from An-poor on their inner sides (zone X in Figs. 4, 5; $An_{50-53}Or_{0.5}$) to An-rich on their outer sides (zone Y in Figs. 4, 5; $An_{53-57}Or_{0.1-0.5}$), resulting in reverse zoning. Sometimes the outermost sides of plagioclase rims, in contact with pyroxene grains, consist of cryptocrystalline intergrowths of plagioclase and pyroxene (zone Z of Fig. 1f). Rarely, zone Z includes small euhedral pyroxene grains which have grown inward from the host pyroxene wall (Fig. 1f). The width of plagioclase rims varies from a few to 50 microns, and zone Z is less than 20 microns in width.

Vesicles, a few microns to several tens of microns across, are often found in Pl-glass or plagioclase rims near boundaries with surrounding minerals (Fig. 1e).

3.5. Chromite

Chromite occurs as euhedral to subhedral grains, ranging in size from a few tens of microns up to 150 microns across. Chemical compositions of all chromites studied here are plotted in Fig. 6. The compositions of chromites in ALH-77005 follow a trend parallel to the tie line connecting the ulvospinel (Us) component with the chromite (Chm) and Al-spinel (Sp) components, but contain a small proportion of the magnetite (Mt) component (Fig. 6).

All chromite grains in ALH-77005 are chemically zoned. There are four types of zoning, which correspond to different textural settings. Chromite inclusions in olivine are Ti-poor, and are zoned from Cr-rich cores (A in Fig. 7a; $Chm_{81}Sp_{14}$-Us_2Mt_3, the Mt component is obtained from stoichiometry) to Cr-poor rims (B in

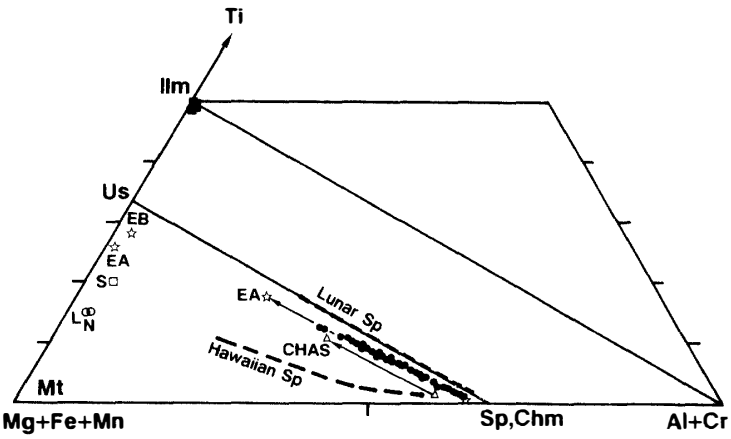

Fig. 6. The Ti–(Al+Cr)–(Mg+Fe+Mn) ratios (in atomic %) of chromites (closed circle) and ilmenites (closed square) in ALH-77005. Chromites and titanomagnetites from other SNC meteorites are shown for reference; EETA79001 lithologires A and B (EA and EB, open star), Chassigny (CHAS, open triangle), Shergotty (S, open square), and Nakhla and Lafayette (N and L, open circle). The compositional ranges of chromites from Lunar basalts (Lunar Sp) and Hawaiian basalts (Hawaiian Sp) are also shown. Abbreviations: Sp (Al-spinel), Chm (chromite), Us (ulvospinel), Mt (magnetite), and Ilm (ilmenite). Data sources: BUNCH and REID (1975), FLORAN et al. (1978), STOLPER and MCSWEEN (1979), MCSWEEN and JAROSEWICH (1983), and Basaltic Volcanism Study Project (1981). There is a compositional gap between Ti-rich chromite and titanomagnetite.

Fig. 7a; $Chm_{74}Sp_{19}Us_4Mt_3$), although one chromite grain in olivine has a Ti-rich rim (Fig. 7a). Chromite in magnesian low-Ca pyroxene is also Ti-poor but Cr-richer than chromite in olivine, ranging from Cr-rich cores (C in Fig. 7b; $Chm_{83}Sp_{12}Us_2Mt_3$) to Cr-poor rims (D in Fig. 7b; $Chm_{78}Sp_{16}Us_3Mt_3$), although one chromite grain in magnesian low-Ca pyroxene has a rim slightly enriched in Al and Ti (Fig. 7b). Chromite in ferroan low-Ca pyroxene, high-Ca pyroxene, and Pl-glass ranges from Ti-poor cores (E in Fig. 7c; $Chm_{80-82}Sp_{13-14}Us_{2-3}Mt_3$) to Ti-rich rims (G in Fig. 7c; $Chm_{44-46}Sp_{10-13}Us_{36-41}Mt_5$). However, one chromite grain in ferroan low-Ca pyroxene has unusual zoning; one half of the grain shows a main trend from a Ti-poor core (E in Fig. 7c) to a Ti-rich rim (G), but the other half has zoning from a Ti-poor rim (E) to a Ti-Al-rich rim (F).

The MgO contents of chromite A–B are nearly constant at 3.5–5.0 wt% (Fig. 8b). Chromites C–D are also nearly homogeneous in MgO in each grain, but differ from grain to grain, ranging from 5 to 7.5 wt% MgO (Fig. 8b). The MgO contents of chromites E–G are nearly constant at 4–5 wt%, although MgO in chromites E–F increases from core at 4.5 wt% to rims at 5.5 wt% (Fig. 8a). The MnO contents of chromite are 0.3–0.8 wt% (Fig. 2).

3.6. *Ilmenite, phosphate, and sulfide*

Ilmenite occurs in the non-poikilitic portion in close association with Pl-glass and whitlockite (Fig. 1g), or as rims on Ti-rich chromite grains. It contains 4.5–6.5 wt% MgO and 0.6–1.0 wt% Cr_2O_3. The MnO content of ilmenite is 0.6–0.9 wt%

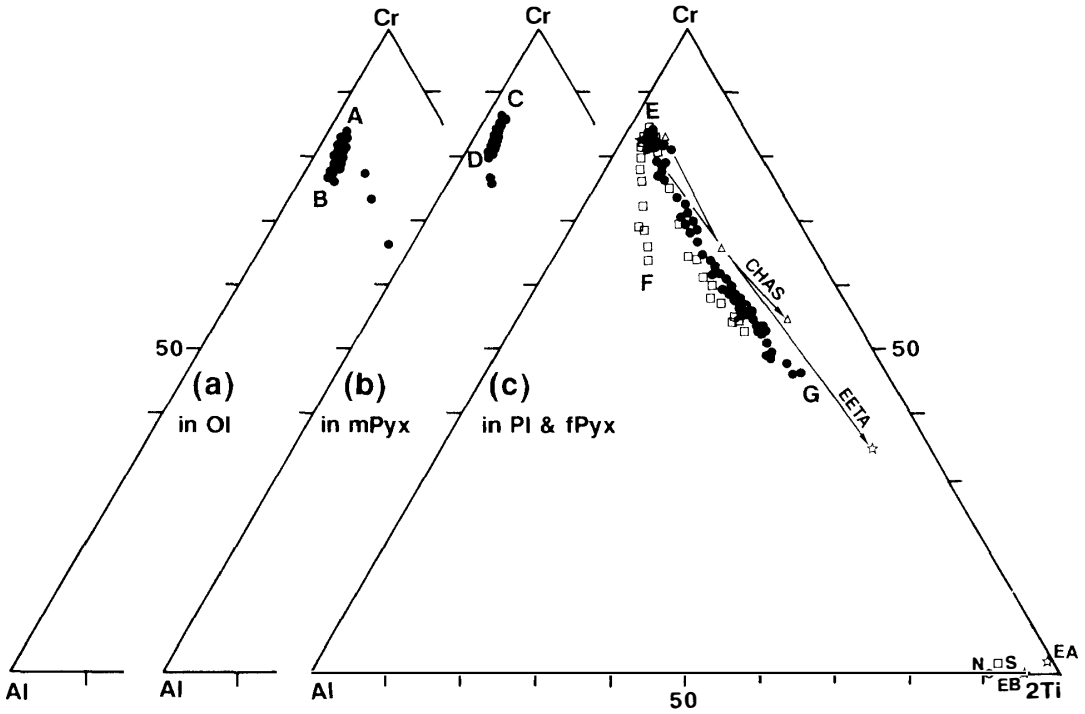

Fig. 7. The atomic ratios of Cr (chromite), Al (Al-spinel), and 2Ti (ulvospinel) for chromites (closed circle and open squares) in ALH-77005. (a) Chromites with zoning from A to B, included in brown olivine, (b) chromites with zoning from C to D, included in magnesian low-Ca pyroxene, and (c) chromites with zoning from E to G, included in plagioclase glass, ferroan pigeonite, and/or augite. A chromite grain (open square), included in ferroan pigeonite, shows unusual zoning from the core (E) to the rim (G and F). The compositional trends of chromites in EETA79001(A) (EETA, open star) and Chassigny (CHAS, open triangle), and the compositions of titanomagnetites in EETA79001(A and B) (EA and EB, open star), Shergotty (S, open square), and Nakhla (N, open circle) are shown for reference. Data sources are the same as those in Fig. 6.

(Fig. 2).

The phosphate in ALH-77005 is whitlockite; large whitlockite grains are partially decomposed but seem to have not fused by shock (Fig. 1g). On the other hand, small whitlockite grains, about 10 microns across, included in Pl-glass are not broken.

Sulfide grains, 100 microns in diameter or smaller, occur as inclusions in olivine, pyroxene, and Pl-glass. They are mainly pyrrhotite, and include small pentlandite grains (about 1 micron across) which may have exsolved from the host pyrrhotite (Fig. 1h).

3.7. Shock-melt pockets and veins

Shock-melt pockets (Fig. 1i), 0.5–3 mm in diameter, are irregular or rounded in outline, and have a halo (Fig. 1i, k) of less than 1 mm width. Shock-melt veins (Fig. 1q, r) are found, especially near the shock-melt pockets, and the width is less than 0.5 mm.

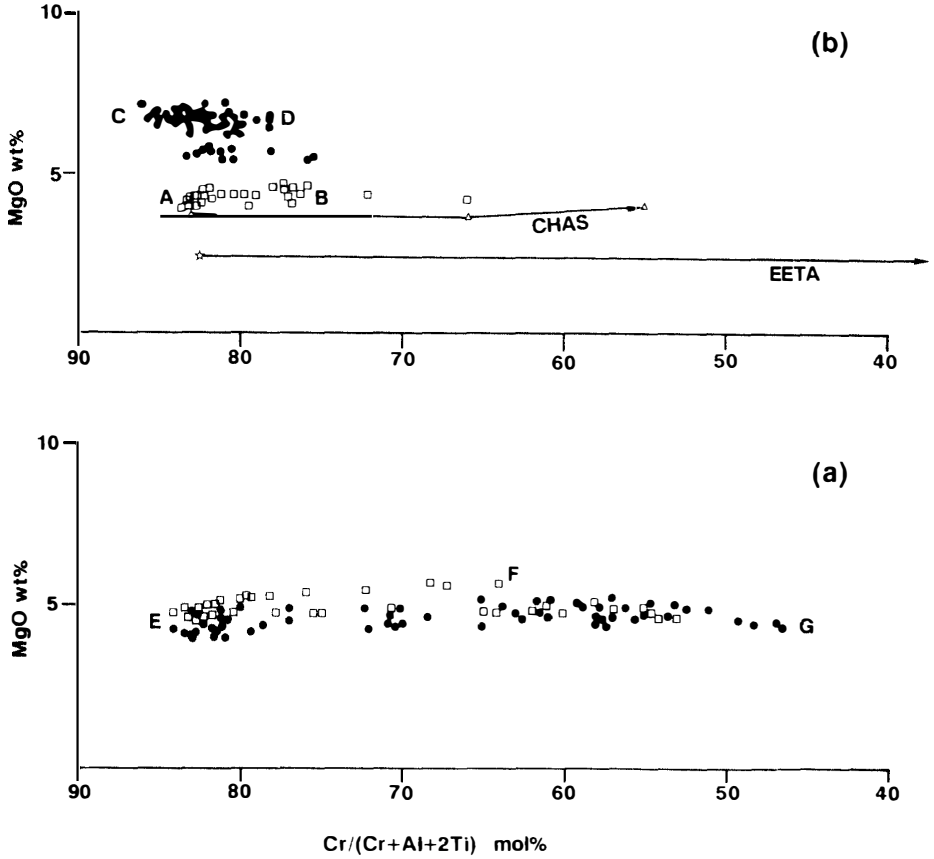

Fig. 8. The MgO contents of chromites in ALH-77005 are plotted against the Cr/(Cr + Al + 2Ti) mole ratios. (a) Chromites with zoning of E–G and G–E–F correspond to those in Fig. 7c, (b) chromites with zoning of A–B (open square) and C–D (closed circle) corrrespond to those in Figs. 7a, b, respectively. The compositional zoning trends for EETA79001(A) (EETA; McSween and Jarosewich, 1983) and Chassigny (CHAS, Floran et al., 1978) are shown for reference.

Shock-melt pockets consist mainly of quenched olivine and interstitial cryptocrystalline materials (Fig. 1i, k, m, n). The quenched olivine is often needle-shaped crystals but sometimes small rhombohedral crystals in cores of some shock-melt pockets (Fig. 1m). The interstitial cryptocrystalline materials are similar in texture to zone Z of the plagioclase rims, mentioned in Section 3.4, and comprise both plagioclase and pyroxene components.

Relict olivine grains are often observed in shock-melt pockets, and have an unusual texture; they look like spherulitic or sheaf-like aggregates under a microscope and are more magnesian (Fo_{75}–Fo_{80}) on average than the brown olivine. Back-scattered-electron (BSE) images (Fig. 1m) show small olivine domains, a few microns across, arranged to form a spherulitic or sheaf-like texture. Each small domain is zoned from a magnesian core to a ferroan rim. Small euhedral olivine grains grow outward from the rims of relict olivine grains (Fig. 1m).

In halos surrounding shock-melt pockets, the crystal structures of olivine and pyroxene are severely modified (Fig. 1j, l, n), and the brownish color of olivine is

lost there. The inner portions of the halos show a domain texture similar to that of relic olivine grains (Fig. 1m).

In a brecciated portion in contact with a shock-melt pocket, long spinifex or lantern-shaped olivine crystals (Fig. 1o), up to 80 microns in length and about 10 microns in width, and small (< 10 microns) grains of pyroxene are observed in cryptocrystalline materials. Near a shock-melt pocket, quenched augite crystals, 20–40 microns in length, grow from the original augite (Fig. 1p).

Shock-melt veins also consist mainly of quenched olivine and interstitial cryptocrystalline materials with minor relic minerals. The quenched olivine is sometimes small euhedral crystals (Fig. 1q) or needle crystals; sometimes they show a lantern or skeletal texture (Fig. 1r). The interstitial cryptocrystalline materials seem to consist of pyroxene and plagioclase.

4. Discussion

4.1. Crystallization sequence and conditions

ALH-77005 is a cumulate gabbroic rock and its crystallization sequence is summarized in Fig. 9, which is consistent with the sequence obtained by LUNDBERG *et al.* (1990). Olivine grains are included in magnesian low-Ca pyroxene in the poikilitic portion, and may have been the liquidus phase. The olivines often show rounded outlines, suggesting that they reacted with their coexisting magma to have produced the host low-Ca pyroxene. However, olivine in the non-poikilitic portion has euhedral or subhedral forms and it seems to have grown without detectable reaction with the coexisting intercumulus liquid.

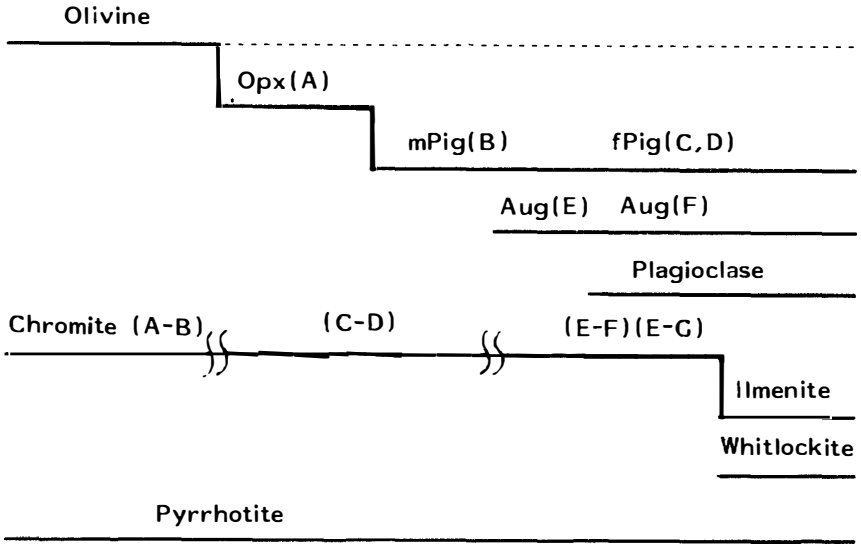

Fig. 9. The sequence of the ALH-77005 crystallization from the left hand side to the right hand side. The capitals in parentheses correspond to those in Fig. 3 for pyroxenes and those in Fig. 7 for chromites.

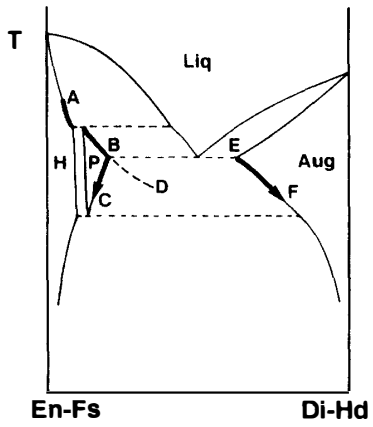

Fig. 10. Schematic phase relation for pyroxenes in ALH-77005. The capitals (A, B, C, D, E, and F) correspond to those in Fig. 3. Stable fields of hypersthene (H), pigeonite (P), augite (Aug), and liquid (Liq) are shown. Abbreviations: temperature (T), enstatite (En), ferrosilite (Fs), diopside (Di), and hedenbergite (Hd).

Pyroxene grains in ALH-77005 show chemical zoning, as shown in Fig. 2; the first crystallizing pyroxene is CaO-poor low-Ca pyroxene (Fig. 2) and may have been orthopyroxene (ISHII *et al.*, 1979) as suggested in Fig. 10. Pigeonite followed orthopyroxene and changed in composition to magnesian pigeonite B (Figs. 2, 10), where CaO-poor augite E (Figs. 2, 10) joined with pigeonite B. Pigeonite B and augite E crystallized together and changed to pigeonite C and augite F (Figs. 2, 10), respectively. Some pigeonite grains seem to have crystallized metastably toward D in Figs. 2 and 10. The pyroxene geothermometry (LINDSLEY and ANDERSON, 1983) gives an equilibrium temperature of about 1200°C for pairs of pigeonite (B in Figs. 2, 10; Table 1) and augite (E in Figs. 2, 13; Table 1) which are in contact, and it is slightly higher than the temperature (1160°C) obtained by ISHII *et al.* (1979). The existence of pigeonite indicates that ALH-77005 has experienced rapid cooling after the crystallization of pigeonite to prevent the inversion to orthopyroxene and formation of exsolution lamellae in pyroxenes. A possible geological setting for this meteorite is as a cumulate rock in a lava lake.

Chromite grains occur in olivine, pyroxene, and plagioclase, indicating that they crystallized at all stages of the ALH-77005 crystallization, except for the very last stage when ilmenite crystallized instead of chromite (MCSWEEN *et al.*, 1979a). Chromite included in olivine has A–B zoning, but that in magnesian low-Ca pyroxene has C–D zoning (Figs. 7, 8). In spite of the earlier crystallization of chromite A–B than chromite C–D, the latter is more enriched in Cr_2O_3 and MgO than the former. This may be explained by the hypothesis that magma mixing took place in a magma reservoir. First, a magma rich in MgO with a high Cr/Al ratio intruded into a magma reservoir which was crystallizing olivine and chromite A–B. This Mg-rich magma crystallized chromite C–D, and reacted with olivine to produce megacrystic magnesian low-Ca pyroxene grains. These composite olivine-chromite aggregates then settled to the bottom of the reservoir (lave lake) to form the poikilitic portion of ALH-77005. At the same time, olivine including chromite A–B and small (smaller than 1 mm) low-Ca pyroxene including chromite C–D settled to form the non-poikilitic portion, with more abundant interstitial liquid from which chromites E–G or E–F crystallized. An alternative hypothesis is that

crystallization conditions changed abruptly between the crystallization of chromites A–B and C–D. Perhaps a magma was crystallizing olivine and chromite A–B in a deep magma chamber. Then, it erupted to the surface, lost its vapor components, and crystallized chromite C–D and magnesian low-Ca pyroxene instead of olivine and chromite A–B. Then these crystal aggregates settled with intercumulus liquid from which chromite E–G or E–F crystallized. The second hypothesis may not be what happens in the case of ALH-77005, because olivine in ALH-77005 crystallized rapidly (JAGOUTZ, 1989).

From the intercumulus liquid, plagioclase crystallized together with ferroan pigeonite, augite, and chromite E–G. The plagioclase glass without plagioclase rims in ALH-77005 is An_{45}–$An_{55}Or_{1\text{-}2}$ (mainly An_{50}–An_{55}), which is similar to, but narrower in compositional range than, those of EETA79001(A) (An_{50}–An_{65} $Or_{0.5}$–$Or_{2.0}$; MCSWEEN and JAROSEWICH, 1983). The original compositions of ALH-77005 plagioclase may have had a wider compositional range than that of the plagioclase glass without plagioclase rims, and may have been homogenized during melting by shock. The chromites in ALH-77005 have the same magnetite content as those in EETA79001(A) (Fig. 6), which is lower than that in Chassigny and higher than those in Lunar basalts (Fig. 6). The oxygen fugacity for ALH-77005 may have been the same as that for EETA79001 (the QFM buffer; MCSWEEN and JAROSEWICH, 1983). The E–G trend for ALH-77005 chromite is similar to the trend for EETA79001(A) chromite (Fig. 7c), although the MgO contents of the former are slightly higher than those of the latter (Fig. 8b). A chromite grain with both E–G and E–F zonings (Fig. 7c) is included in ferroan pigeonite. The E–F zoning may have been due to a local phenomena where Al_2O_3 was enriched locally by rapid crystallization of ferroan low-Ca pyroxene grains surrounding the E–F chromite grain. An olivine grain includes a chromite grain having zoning similar to the earlier half of E–G zoning (Fig. 7a), suggesting that olivine might have crystallized locally from the interstitial liquid in the non-poikilitic portion. Adcumulative growth processes of olivine and/or pyroxene might have taken place in the cumulate. Whitlockite and ilmenite were products of the latest stage crystallization (MCSWEEN *et al.*, 1979a). Pyrrhotite occurs in olivine, pyroxene, and plagioclase, and seems to have crystallized throughout the ALH-77005 crystallization. Pentlandite was produced by exsolution of Ni-bearing pyrrhotite, probably under a subsolidus condition.

JAGOUTZ (1989) found silica-rich inclusions trapped in brown olivines, suggesting a rapid growth origin of the brown olivines. Therefore, ALH-77005 was produced as autolithic cumulus phases with the intercumulus liquid. The brown olivines, magnesian low-Ca pyroxene, and Ti-poor chromites in ALH-77005 were originally cumulates which may have been produced by fractionation and mixing of basaltic magmas in a rapid cooling condition at a shallow level. The crystallization age is about 150–160 Ma (JONES, 1986; JAGOUTZ, 1989).

4.2. *Zonation of plagioclase glass and the rims*

After the consolidation, ALH-77005 experienced the most intense shock effects

among all of the SNC meteorites (LAMBERS, 1985; BISCHOFF and STOFFLER, 1992). The original plagioclase grains were changed to plagioclase melts by the intense shock, and plagioclase crystallized from some plagioclase melts near shock-melt pockets (MCSWEEN and STOFFLER, 1980; JAGOUTZ, 1989); plagioclase nucleated at the boundaries with the surrounding olivine or pyroxene, grew inward to form the plagioclase of zone Y (Fig. 5) at the outermost rims, and then the plagioclase of zone X (Fig. 5) crystallized inside zone Y, resulting in the plagioclase rims.

During rapid crystallization of An-rich plagioclase rims, the Ab and Or components of the melts accumulated just inside of crystallization front of the plagioclase rims to form zone W in the plagioclase melts, resulting in the V–W zoning of the melts (Fig. 5). The rapid cooling of ALH-77005 has caused the melts to have quenched to form the zoned Pl-glass. The An component of plagioclase X (about An_{50}) which crystallized from plagioclase melt W (about An_{40}) is too low in comparison with those (about An_{75}) crystallizing in equilibrium with such a melt, indicating that the plagioclase rims crystallized under a supercooled condition.

Zone Z is sometimes observed between plagioclase rims and the surrounding pyroxene, and consists of a cryptocrystalline mixture of plagioclase and pyroxene (Fig. 1f). The zone may have been produced from a melt having both pyroxene and plagioclase components, which was produced by fusion of the pyroxene in direct contact with plagioclase melts; the melt crystallized small euhedral pyroxenes which grew from the surrounding pyroxene wall (Fig. 1f), and then a cryptocrystalline mixture was produced by parallel growth (Fig. 1f), resulting in zone Z prior to the crystallization of zone Y.

Melting of plagioclase requires more than 50–60 GPa shock pressures, which correspond to peak-shock temperatures of 1700–2700°C (BISHOFF and STOFFLER, 1992), and the post-shock temperature may have been higher than the melting point of ALH-77005 plagioclase (about 1450°C). Pl-glass in ALH-77005 is commonly associated with small vesicles near the boundaries with the surrounding silicates (Fig. 1e), and these vesicles may have formed by such high temperatures. However, the shock pressures of 50–60 GPa, estimated for formation of plagioclase melts, correspond to peak-shock temperatures of about 600–800°C for forsteritic olivine (BISHOFF and STOFFLER, 1992), suggesting that most of the olivine and pyroxene could not be fused by such a shock pressure. This is consistent with the facts that all of the original plagioclase changed to melt without remarkable melting of olivine and pyroxene in ALH-77005, except for shock-melt pockets and veins, and that most of the plagioclase melts that were produced quenched as glass.

4.3. Shock-melt pockets and veins

Chemical compositions of shock-melt pockets (Fig. 11) are enriched in the olivine component in comparison with the ALH-77005 whole rock composition, but have a constant plagioclase content similar to that of the whole rock composition. This suggests that shock-melt pockets were produced locally and preferentially from olivine-rich portions; shock impact energy had locally concentrated in small por-

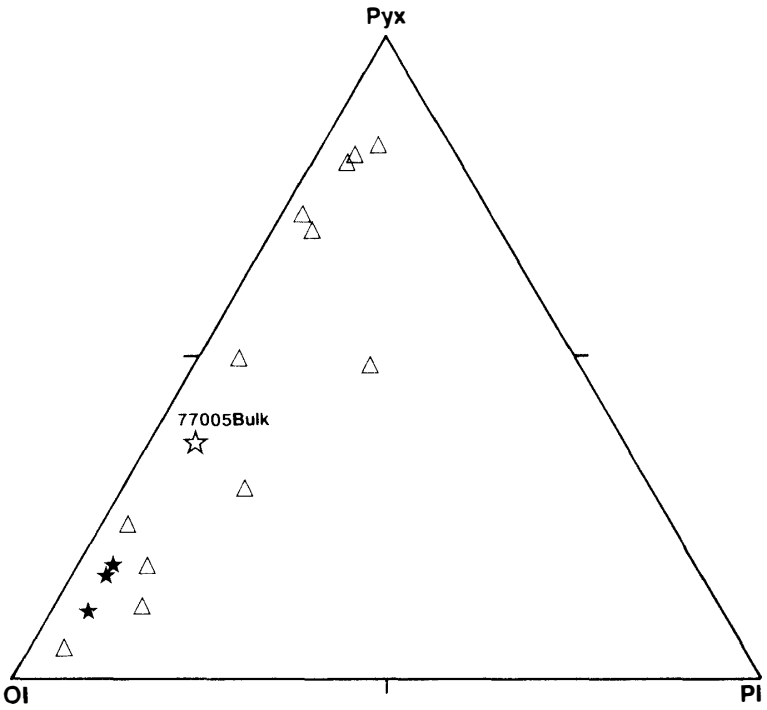

Fig. 11. Normative compositions (in mole%) of shock-melt pockets (closed star) and veins (open triangle) in ALH-77005. Pyx, Ol, and Pl are normative pyroxene (Wo+En +Fs), olivine (Fo+Fa), and plagioclase (An+Ab+Or) components. The composition of the ALH-77005 whole rock (SHIH et al., 1982) is shown for reference.

tions enriched in olivine, a few mm or small in diameter, with minor amounts of plagioclase and pyroxene, and they were fused to produce shock-melt pockets, whereas pyroxene-predominant portions were not fused enough to produce shock-melt pockets. Bulk melting of olivine with minor plagioclase and pyroxene requires shock pressures of about 80 GPa (MCSWEEN and STOFFLER, 1980; BISHOFF and STOFFLER, 1992), which may have been due to localized stress concentration. The halos surrounding shock-melt pockets (Fig. 1k, l, n) present evidence for the *in-situ* melting; the halos have experienced more intense shock than the host surrounding the halos (Fig. 1l, n). The domain texture of olivine in halos consists of small elliptical domains, and each domain has normal zoning (Fig. 1n). Shock experiments for dunite chips (HEYMANN and CELLUCCI, 1988) revealed that high shock pressures of about 60 GPa formed olivine glass with a considerable degree of three-dimensional Si-O-Si linkage, having scattered domains. Therefore, the domain texture of olivine in halos near shock-melt pockets and veins in ALH-77005 may be due to the high shock pressure of about 60 GPa. An augite grain in contact with a shock-melt pocket has been fused at the rim to produce an augite melt, and the melt crystallized quenched augite crystals (Fig. 1p), supporting the *in-situ* melting.

Shock-melt veins in ALH-77005 have a wide compositional range in comparison to shock-melt pockets (Fig. 11); some portions of veins are dominated by pyroxene components, and others by olivine components with varying amounts of

plagioclase. They also may have been produced by local stress concentration, but the chemical compositions of the veins do not necessarily correspond to the host minerals intercalating the veins (Fig. 1r), suggesting that the vein melts moved slightly prior to the final consolidation.

The shock pressures of 50–80 GPa which are required for melting of ALH-77005 plagioclase and the formation of shock-melt pockets correspond to impact velocity of 3–6 km/s for a basaltic (or dunitic) target-basaltic (or iron) projectile pair (STOFFLER *et al.*, 1988). ALH-77005 may have been ejected from Mars by the shock. The shock age of ALH-77005 is less than 20 Ma (JAGOUTZ, 1989), and the exposure age is 2.7 Ma (NISHIIZUMI *et al.*, 1986).

5. Conclusions

(1) Chromite in ALH-77005 has four types of chemical zoning, which correspond to the differences in occurrence. The compositional discontinuity among the zoning types may suggest magma mixing in a shallow magma reservoir such as a lava lake on Mars.

(2) Plagioclase glass has sometimes plagioclase rims, and these rims were produced from plagioclase melts by rapid crystallization.

(3) Shock-melt pockets were produced by *in-situ* melting of olivine-rich portions, where shock stress was concentrated locally. The ubiquitous occurrence of the shock-melt pockets and plagioclase melts requires shock pressures ranging from 50–80 GPa.

Acknowledgments

I thank Drs. K. YANAI and H. KOJIMA of the National Institute of Polar Research, the ANSMET program and the Curator of Antarctic Meteorites of Johnson Space Center for the sample preparation, Dr. J. DELANEY for discussion, and Drs. A. H. TREIMAN and H. Y. MCSWEEN, Jr. for constructive comments that improved this manuscript. This study was supported by a Grant-in-Aid for Scientific Research, from the Ministry of Education, Science, and Culture.

References

BASALTIC VOLCANISM STUDY PROJECT (1981): Basaltic Volcanism on the Terrestrial Planets. New York, Pergamon Press.

BISHOFF, A. and STOFFLER, D. (1992): Shock metamorphism as a fundamental process in the evolution of planetary bodies: Information from meteorites. Eur. J. Mineral., **4**, 707–755.

BOGARD, D. D., NYQUIST, L. E. and JOHNSON, P. (1984): Noble gas contents of shergottites and implications for the Martian origin of SNC meteorites. Geochim. Cosmochim. Acta, **48**, 1723–1739.

BUNCH, T. E. and REID, A. M. (1975): The nakhlites Part 1: Petrography and mineral chemistry. Meteoritics, **10**, 303–324.

FLORAN, R. J., PRINZ, M., HLAVA, P. F., KEIL, K., NEHRU, C. E. and HINTHORNE, J. R. (1978): The Cassigny meteorite: A cumulate dunite with hydrous amphibole-bearing melt inclusions.

Geochim. Cosmochim. Acta, **42**, 1213–229.

HARVEY, P. and MCSWEEN, H. Y., Jr. (1992): The mineralogy and petrology of LEW88516 (abstract). Meteoritics, **27**, 231–232.

HEYMANN, D. and CELLUCCI, T. A. (1988): Raman spectra of shocked minerals 1: Olivine. Meteoritics, **23**, 353–357.

IKEDA, Y. (1980): Petrology of Allan Hills-764 chondrite (LL3). Mem. Natl Inst. Polar Res., Spec. Issue, **17**, 50–82.

ISHII, T., TAKEDA, H. and YANAI, K. (1979): Pyroxene geothermometry applied to a three-pyroxene achondrite from Allan Hills, Antarctica and ordinary chondrites. Mineral. J., **9**, 460–481.

JAGOUTZ, E. (1989): Sr and Nd isotopic systematics in ALHA77005: Age of shock metamorphism in shergottites and magmatic differentiation on Mars. Geochim. Cosmochim. Acta, **53**, 2429–2441.

JONES, J. H. (1986): A discussion of isotopic systematics and mineral zoning in the shergottites: Evidence to 180 Ma igneous crystallization. Geochim. Cosmochim. Acta, **50**, 969–977.

LAMBERT, P. (1985): Metamorphic record in shergottites. Meteoritics, **20**, 690–691.

LINDSLEY, D. H. and ANDERSON, D. J. (1983): A two-pyroxene thermometer. Proc. Lunar Planet. Sci. Conf., 13th, Part 2, A887–A906 (J. Geophys. Res., **88** Suppl.).

LONGHI, J. and PAN, V. (1989): The parent magmas of the SNC meteorites. Proc. Lunar Planet. Sci. Conf., 19th, 451–464.

LUNDBERG, L. L., GROZAZ, G. and MCSWEEN, H. Y., Jr. (1990): Rare earth elements in minerals of the ALHA77005 shergottite and implications for its parent magma and crystallization history. Geochim. Cosmochim. Acta, **54**, 2535–2547.

MA, M. S., LAUL, J. C. and SCHMITT, R. A. (1981): Analogous and complimentary rare earth element patterns on meteorite parent bodies and the earth infered from a study of the achondrite ALHA77005. Lunar and Planetary Science XII. Houston, Lunar Planet. Inst., 634–636.

MCSWEEN, H. Y., Jr. (1984): SNC meteorites: Are they Martian rocks? Geology, **12**, 3–6.

MCSWEEN, H. Y., Jr. (1985): SNC meteorites: Clues to Martian petrologic evolution? Rev. Geophys., **23**, 391–416.

MCSWEEN, H. Y., Jr. and JAROSEWICH, E. (1983): Petrogensis of the Elephant Moraine A79001 meteorite: Multiple magma pulses on the shergottite parent body. Geochim. Cosmochim. Acta, **47**, 1501–1513.

MCSWEEN, H. Y., Jr. and STOFFLER, D. (1980): Shock metamorphic features in Allan Hills 77005 meteorite. Lunar and Planetary Science XI. Houston, Lunar Planet Inst., 717–719.

MCSWEEN, H. Y., Jr., TAYLOR, L. A. and STOLPER, E. M. (1979a): Allan Hills 77005: A new meteorite type found in Antarctica. Science, **204**, 1201–1203.

MCSWEEN, H. Y., Jr., STOLPER, E. M., TAYLOR, L. A., MUNTEAN, R. A., O'KELLEY, G. D., ELDRIDGE, J. S., BISWAS, S., NGO, H. T. and LIPSCHUTZ, M. E. (1979b): Petrogenetic relationship between Allan Hills 77005 and other achondrites. Earth Planet. Sci. Lett., **45**, 275–284.

NISHIIZUMI, K., KLEIN, J., MIDDLETON, R., ELMORE, D., KUBIK, P. W. and ARNOLD, J. R. (1986): Exposure history of shergottites. Geochim. Cosmochim. Acta, **50**, 1017–1021.

OSTERTAG, R., AMTHAUER, G., RAGER, H. and MCSWEEN, H. Y., Jr. (1984): Fe^{+3} in shocked olivine crystals of the ALHA77005 meteorite. Earth Planet. Sci. Lett., **67**, 162–166.

SHIH, C. Y., NYQIST, L. E., BOGARD, D. D., MCKAY, G. A., WOODEN, J. L., BANSAL, B. M. and WEISMANN, H. (1982): Chronology and petrogenesis of young achondrites, Shergotty, Zagami, and ALHA77005: Late magmatism on a geological active planet. Geochim. Cosmochim. Acta, **46**, 2323–2344.

SMITH, J. V. and STEELE, I. M. (1984): Achondrite ALHA77005: Alteration of chromite and olivine. Meteoritics, **19**, 121–133.

STOFFLER, D., OSTERTAG, R., JAMMES, C., PFANNSCHMIDT, G., SEN GUPTA, P. R., SIMON, S. B., PAPIKE, J. J. and BEAUCHAMP, R. H. (1986): Shock metamorphism and petrography of the Shergotty achondrite. Geochim. Cosmochim. Acta, **50**, 889–903.

STOFFLER, D., BISCHOFF, A., BUCHWALD, V. and RUBIN, A. E. (1988): Shock effects in meteorites. Meteorites and the Early Solar System, ed. by J. F. KERRIDGE and M. S. MATHEWS. Tucson, Univ. Arizona Press, 165–202.

STOLPER, E. and MCSWEEN, H. Y., Jr. (1979): Petrology and origin of the shergottite meteorites. Geochim. Cosmochim. Acta, **43**, 1475–1498.

(Received August 4, 1993; Revised manuscript received October 19, 1993)